Automated T2* Mapping with Susceptibility Removal for the Assessment of Cardiac Iron Content

Brian A. Taylor[1], Ralf B. Loeffler[1], Ruitian Song[1], Mary E. McCarville[1], Jane S. Hankins[2], and Claudia M. Hillenbrand[1]

[1]*Radiological Sciences, St. Jude Children's Research Hospital, Memphis, Tennessee, United States,* [2]*Hematology, St. Jude Children's Research Hospital, Memphis, Tennessee, United States*

Introduction: Hematological conditions such as β-thalassemia major and sickle cell disease often require blood transfusions for disease management. Heavy iron accumulation in the heart can occur from multiple transfusions and can lead to life-threatening conditions such as arrhythmias and impaired left ventricular function [1-4]. One of the most commonly used methods for noninvasive cardiac iron measurements is T_2* mapping of the mid-papillary short axis of the left ventricle, where low T2* values (<20 ms) are indicative of a higher risk of iron-induced cardiac complications [2-4]. Typically, T_2* measurements are made in a region of interest (ROI) in the intraventricular septum (IS) to avoid T_2*-lowering susceptibility effects from lung, liver, and epicardial fat [5]. In this work, we implemented and evaluated an automated method that incorporates an autoregressive moving average (ARMA) model [6] of the complex signal from a multi-gradient echo (mGRE) acquisition to map the field and T_2* of the whole left ventricle (LV). Using the field map, areas of high susceptibility due to various causes including air/tissue interfaces, deoxygenated blood in the cardiac veins and epicardial fat are identified and extracted without additional user input for automated ROI analysis in the T_2* based assessment of cardiac iron.

Methods: Twenty-four patients with suspected iron overload were scanned in accordance to an IRB-approved protocol. All patients were examined on a 1.5T scanner and mGRE short-axis images were obtained in a single breath-hold. Echo times (TE) ranged from 1.5ms to 21.3ms at 1.8ms increments (ETL 12). Other imaging parameters were: flip angle 25º, slice thickness 8mm, matrix 128 × 128 and FOV 300-400mm depending on the patient size. Magnitude and phase images were obtained as inputs for the ARMA algorithm, which then calculates the chemical shift and T_2* by assuming a linear combination of complex exponentials with noise. This algorithm characterizes the signal as a rational polynomial in the *z*-domain via the z-transform and the poles of the polynomial corresponds to the field and T_2*[6]. A ROI was selected encompassing the entire LV. This is the only user interaction needed for the T_2* calculation. From these field gradient values in the ROI, the median gradient was obtained and all voxels with gradients above the median were excluded from the final ROI and T_2* calculation, respectively. Next, the algorithm identified extraneous voxels that are not connected to other voxels and omitted them from the T_2* calculation. The ARMA-fitted T_2* values of the remaining area are used to obtain mean values and standard deviations (std) for T_2* in the LV.

Table 1

	T2* (ms)	CoV	% of LV
LV	28.6 ± 6.0	0.49+ ± 0.08	
IS	35.1 ± 10.0 *	0.33 ± 0.13 **	21.1 ± 3.4
ARMA	32.6 ± 7.0 *	0.31 ± 0.06 **	39.8 ± 5.4 ***

* Statistically Different from LV T2* (p<0.01)

** Statistically Different from LV CoV (p<0.001)

*** Statistically Different from IS % Vol (p<0.0001)

Table 2

Region	Percent of Voxels Excluded for Susceptibility	CoV Before Correction	CoV After Correction
IS	31.1 ± 15.1	0.48 ± 0.15	0.26 ± 0.09*
AW	53.6 ± 19.2	0.47 ± 0.19	0.23 ± 0.08*
LFW	86.0 ± 16.8	0.79 ± 0.34	0.25 ± 0.12**
PIW	68.3 ± 26.7	0.55 ± 0.21	0.28 ± 0.14*

Anterior wall (AW), lateral free wall (LFW), posterior/inferior wall (PIW)
* p<0.01 **p<0.001

Results: Table 1 outlines the mean T_2* measurements between the entire LV, IS, and ARMA-defined regions over all 24 patients. There was no statistical difference in the mean T_2* values between the IS and ARMA regions (p=0.31). The population mean T_2* of the entire LV was lower than the T_2* measurement from the two ROIs (IS and ARMA) (p<0.01). The mean (std) IS ROI volume was 21.1% (3.4%) of the volume of the left ventricle. In comparison to the IS volume, the volume for T_2* measurements defined by the ARMA model was 39.8 (5.5%) (p<0.0001) of the whole LV. Although, on average, the volume for the ARMA-defined region was significantly higher, the coefficient of variation (CoV) of the T_2* measurements between the IS and ARMA did not differ from the IS CoV. Compared to the LV CoV, there was an 18% decrease in the CoV calculated by the ARMA technique (p<0.0001). In evaluating the four regions of the LV, there were areas where susceptibility was consistently high in our patient cohort regardless of iron-overload. Table 2 displays which areas were used for ARMA-defined T_2* measurements, which corroborates with other studies investigating T_2* variations in the LV [7,8]. An example of the regions selected by the ARMA method is shown in figure 1. As shown in [7,8], the IS had the least susceptibility as seen in figure 1.

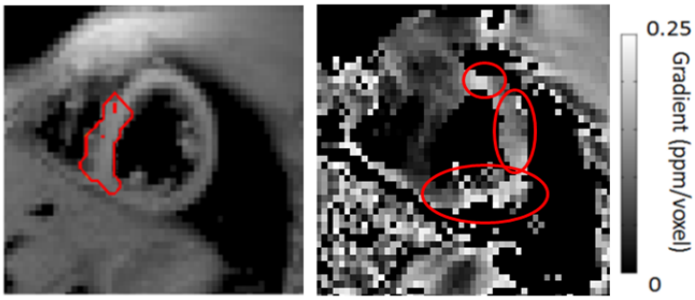

Figure 1: An example of an area selected by the ARMA algorithm. High susceptibility was automatically detected in parts of the AW, LFW, and PIW (circles in right figure). This made the IS the area of least susceptibility for T_2* measurements.

Discussion: By using the field map provided by the ARMA model of the mGRE acquisition, areas of high susceptibility not due to iron were automatically identified and removed to reduce the T_2* variation in the left ventricle. With this technique, T_2* values were reported with higher precision providing more volume for T_2* measurements than with conventional manual segmentation. With this method, the user only outlines the LV, then the T_2* is automatically calculated in areas where susceptibility from various sources is relatively minimal. Therefore, this method shows potential in reducing bias in manually-selected T_2* measurements for iron overload assessment.

References: [1] Borgna-Pignatti C, et al. Ann N Y Acad Sci 2005, 1054:40-47. [2] Anderson LJ, et al. Eur Heart J 2001, 22:2171-2179. [3] Kirk P, et al. Circulation 2009, 120:1961-1968. [4] Wood JC, et al. Circulation 2005, 112:535-543. [5] Wood JC, Noetzli L. Ann N Y Acad Sci 2010, 1202:173-179. [6] Taylor BA, et al. Med Phys 2009, 36:753-764. [7] Yamamura J, et al. J Magn Reson Imaging 2010, 32:1104-1109. [8] Meloni A, et al. Magn Reson Med 2010, 64:211-219.